Magnetic behavior of Fe x Sn 1 – x amorphous alloys near the critical composition

M. Piecuch, Chr. Janot, G. Marchal, M. Vergnat

Magnetic behavior of Fe_xSn_{1-x} amorphous alloys near the critical composition

M. Piecuch
Laboratoire de Physique du Solide, Laboratoire No. 155 associé au Centre National de la Recherche Scientifique, Université de Nancy I, Boîte Postale 239, F-54506 Vandoeuvre-les-Nancy Cédex, France

Chr. Janot
Institut Laue-Langevin, Boîte Postale 156X, F-38042 Grenoble Cédex, France

G. Marchal and M. Vergnat
Laboratoire de Physique du Solide, Laboratoire No. 155 associé au Centre National de la Recherche Scientifique, Université de Nancy I, Boîte Postale 239, F-54506 Vandoeuvre-les-Nancy Cédex, France

(Received 25 October 1982; revised manuscript received 1 March 1983)

Amorphous alloys of the tin-iron system have been prepared by the vapor-quenching technique. Bulk magnetic data show typical "spin-glass-like" behavior in the low-temperature susceptibility and in the remanent magnetization for alloys containing less than about 40 at. % of iron. A multicritical magnetic phase diagram with paramagnetic, ferromagnetic, and spin-glass-like phases is proposed. High-field magnetization measured up to 150 kOe strongly suggests that local anisotropy, randomly oriented through the material, might successfully compete with exchange interactions for some of the iron clusters.

I. INTRODUCTION

The presence of transition metals in amorphous alloys results in magnetic behavior ranging from diamagnetism to ferromagnetism.[1] Simultaneous presence of different magnetic interactions (ferro- and antiferromagnetism for instance) and/or competition between exchange and local anisotropy may result in the appearance of spin-glass-like or cluster-glass states. Such a behavior has been mostly observed in crystalline nonmagnetic materials containing magnetic impurities[2,3] interacting via the Ruderman-Kittel-Kasuya-Yosida (RKKY) long-range mechanism.[4–6] A number of concentrated alloys containing at least two magnetic species with different near-neighbor interactions in a nonmagnetic host[7] also exhibit a similar behavior, with evidences of spin-glass (SG) ferromagnetic (FM) and reentrant spin-glass (RSG) phases. In the description given by a multicritical phase diagram (Fig. 5) of the sort first predicted by Kirkpatrick and Sherrington[8] the RSG phase is entered via a second-order transition from the FM phase with decreasing temperature. In fact, the existence of such a low-temperature phase transition between FM and SG states has been extensively questioned.[9–11] Similar behavior has been recently observed in both kinds of amorphous systems.[12–16]

The main experimental evidences considered as typical of a spin-glass-like phase can be summarized as follows.

(a) The temperature dependence of the magnetic susceptibility shows a very-well-defined cusp in nearly-zero-field conditions but there is no susceptibility cusp in high-field measurements.[14]

(b) At low temperatures strong hysteretic properties can be measured leading to the definition of a "blocking temperature" T_G.[17,18]

(c) Time-dependent remanence and relaxation are observed.[18,19]

In addition to these rather well-accepted properties, theoretical approaches have also described the SG phase. For instance, the classical RKKY model has led to an analytical expression of the magnetization near saturation of the form[20–22]

$$\frac{\sigma}{\sigma_0}=1-\frac{H_0(T)}{H}\ , \tag{1}$$

with

$$H_0(T)=\frac{A_s k_B T}{g\mu_B}+\frac{2(2S+1)nV_0}{3g\mu_B}$$

[S is the spin of the magnetic impurities whose atomic concentration is n; V_0 is the amplitude of the RKKY potential $V_r=(V_0/r^3)\cos 2k_F r$]. More recently, Parisi *et al.*[23,24] have proposed a mean-field theory predicting a criticality only in the second derivative of the magnetization which can be experimentally tested by plotting magnetic susceptibility versus field near the transition temperature.

In disordered systems (chemically and/or topologically as is mostly the case in amorphous alloys) various magnetic inhomogeneities may be thought of, most of them having common behavior with a spin-glass-like phase. Thus it might be worth summing up the method of comparing the data with other models.

A. Jaccarino-Walker and the cluster models (Ref. 25)

In the Jaccarino-Walker model of the magnetization in concentrated binary alloys, the magnetic atom is supposed to really bear a magnetic moment only when it has a certain minimum number n_0 of magnetic atoms in its nearest-neighbor shell. The model can be tested by comparing data to calculated mean magnetic moments with the formula

$$\bar{\mu}=\sum_{n=n_0}^{N}\mu(n)P(n)\ , \tag{2}$$

$P(n)$ being the probability of finding n magnetic atoms among the N nearest neighbors of a given magnetic atom.

Near the critical composition for the onset of ferromagnetic order in alloys, statistical magnetic clusters may be observed. Then the magnetization will be described by

$$\frac{\sigma}{\sigma_0}=\int P(\mu)\mu\mathscr{L}\left[\frac{\mu H}{k_B T}\right]d\mu\ . \tag{3}$$

$P(\mu)$ is the probability of having clusters with μ magnetic moment and $\mathscr{L}(x)$ is the classical Langevin function in the simplified case of only one kind of cluster.

B. Random anisotropy model (Refs. 1, 26, and 27)

Strong local anisotropy may compete with exchange interaction and, when randomly oriented, results in freezing the magnetic moments in noncolinear structures. Saturation, which becomes very difficult to achieve, is then approached by expressions of the form

$$\frac{\sigma}{\sigma_0}=1-\frac{A}{(H+H_0)^2}\ , \tag{4}$$

A being a constant depending on the anisotropy energy and H_0 an apparent anisotropy field. Plotting $(\sigma_0-\sigma)^{-1/2}$ vs H should then result in straight lines whose slope and intersect with the ordinate axis would give A and H_0 values.

C. Microscopic magnetic inhomogeneities

Magnetic inhomogeneities may be due to defects in the structure or correlation effect in chemical disorder. These various aspects have been investigated in detail.[28–30] The main consequence of microscopic disorders is a curvature in the Arrots plots,

$$\sigma^2=f\left[\frac{H}{\sigma}\right]\ . \tag{5}$$

D. Macroscopic disorder

Inhomogeneity of a magnetic alloy may arise far from the atomic level (segregations, polycrystalline materials, etc.). This may result in space fluctuations $\langle\Delta\sigma^2\rangle$ of the magnetization σ_0 near the saturation condition, so that[31]

$$\sigma=\sigma_0\left[1-\frac{\langle\Delta\sigma^2\rangle}{\sigma_0^{\,2}}f\left[\frac{4\pi\sigma_0}{H}\right]\right] \tag{6}$$

with

$$f(x)=\frac{1}{2}\left[\frac{3+2x}{(x+x^2)^{1/2}}\ln[(1+x)^{1/2}+x^{1/2}]-3\right]\ .$$

Data can be easily tested to the model by plotting $\sigma-\sigma_0$ vs $f(x)$ which would give a straight line in successful cases.

The purpose of the present paper has been to investigate the magnetic behavior of Fe_xSn_{1-x} amorphous alloys in a composition range not too far from the critical iron concentration for the onset of ferromagnetic order. As the corresponding crystalline compounds are either ferromagnetic (Fe_3Sn, Fe_5Sn_3, and Fe_3Sn_2) or antiferromagnetic (FeSn and $FeSn_2$), one may wonder which kind of magnetic structure is able to accommodate both topological disorder and competition between FM and antiferromagnetic (AF) interactions. These iron-tin amorphous alloys can be obtained over quite a large compositional range ($0.10<x<0.72$). Most of their structural and physical properties have been measured and reported elsewhere.[32,33] In particular, it has been shown that bulk magnetization vanishes at a critical composition $x_{cr}\simeq 0.3$ and that the alloys are typical ferromagnets down to $x\simeq 0.40$. This paper will present a detailed analysis of the magnetic data as measured in amorphous Fe_xSn_{1-x} alloys with x not too far from the 0.35–0.45 range (corresponding to AF crystalline compounds) over which magnetic inhomogeneities and/or spin-glass-like states are expected.

II. EXPERIMENTS AND RESULTS

A. Samples and magnetization measurements (Ref. 34)

Amorphous iron-tin films have been prepared by the vapor-quenching technique in ultrahigh-vacuum condi-

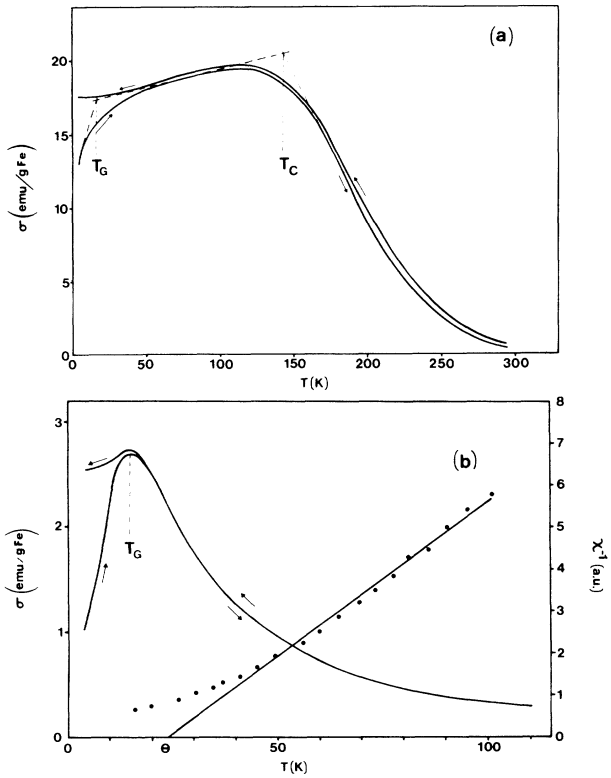

FIG. 1. Typical isofield magnetic curves obtained from various Fe_xSn_{1-x} amorphous alloys where (a) $x=0.43$ and (b) $x=0.33$, with an applied external field $H=100$ Oe. Arrows indicate that $\sigma(T)$ is measured with increasing or decreasing temperatures. In (b) the temperature dependence of the reciprocal susceptibility is also shown. (Hysteresis observed up to 300 K might be an experimental artifact due to difference in heat-transfer velocity when cooling and warming samples.)

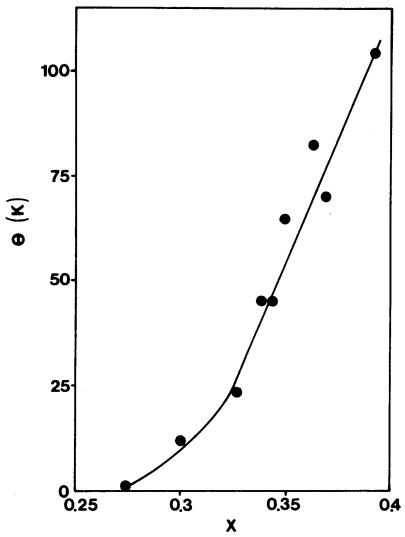

FIG. 2. Compositional dependence of the paramagnetic Curie temperature in the Fe_xSn_{1-x} amorphous alloys.

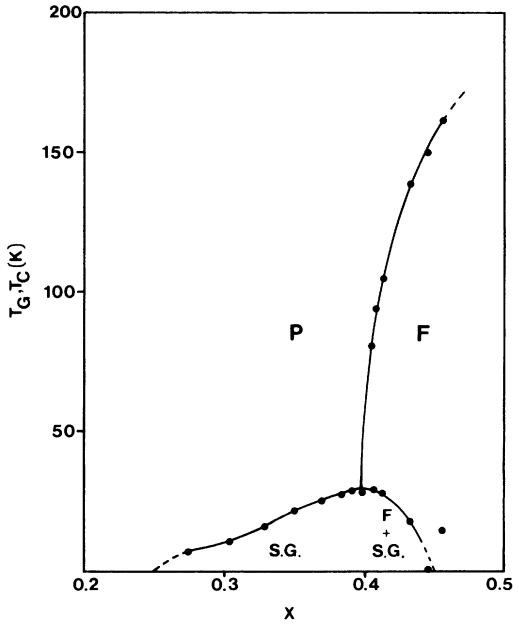

FIG. 4. Tricritical magnetic phase diagram of the Fe_xSn_{1-x} amorphous system: P = paramagnetism, F = ferromagnetism, and SG = spin-glass-like states.

tions. Bulk magnetization data have been measured using either a Foner vibrating-sample magnetometer (up to $H=20$ kOe, including low-field measurements down to $H\simeq 100$ Oe) or the high-field facilities of the "Service National des Champs Intenses" (S.N.C.I.) in Grenoble (up to 150 kOe using a classical extraction method). Magnetic isofield $\sigma(T)$ and magnetic isotherm $\sigma(H)$ curves have been obtained. Suitable samples have been obtained by piling up the evaporated films in a rectangular prism shape ($6\times 12\times 0.7$ mm^3 including substrates), and particular care has been taken to account for demagnetizing field effects as explained in Ref. 34. In particular, it has been checked that the maximum slope $d\sigma/dH$ in a hysteresis loop matches the reciprocal demagnetizing factor for Fe_xSn_{1-x} alloys containing 45 at. % iron or more.[34]

B. Magnetic isofield curves

Thermomagnetic curves have been recorded as described in detail elsewhere.[34] Samples are first demagnetized at room temperature and cooled down to 4.2 K under zero external field. Then the applied magnetic field is set to the constant value $H=100$ Oe and magnetization $\sigma(T)$ is measured while T is increased from 4.2 to 250 K, then decreased from 250 to 4.2 K. Typical isofield curves are shown in Fig. 1 for various typical alloy compositions. Above a certain temperature, a typical paramagnetic behavior can be observed with a linear temperature dependence of the reciprocal susceptibility [see the right-hand-side curve in Fig. 1(c)],

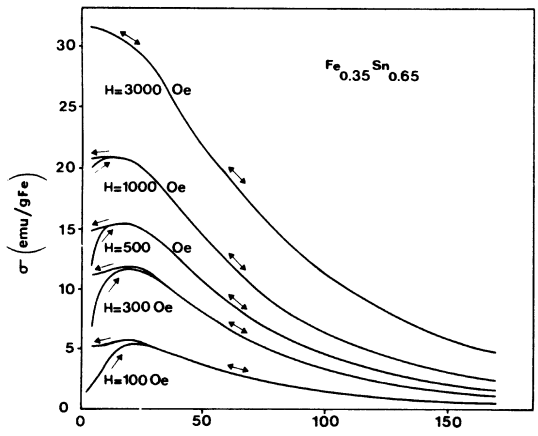

FIG. 3. Set of isofield magnetization curves recorded with different values of the external applied field. The low-temperature irreversible part and the susceptibility maximum are completely suppressed with a field of about 3000 Oe.

TABLE I. Transition temperatures as functions of iron concentrations in the amorphous Fe_xSn_{1-x} alloys.

x	T_G (K)	T_c (K)	Θ (K)
45.6	15	162	178
44.5	<4.2	150	165
43.2	18	139	151
41.3	28	105	129
40.7	29	93	122
40.4	28	81	119
39.2	29		105
38.4	27		68
36.9	25		83
36.2	23.5		63
34.9	22		45
34.0	19		45
32.9	15.8		25
30.4	10.3		10
27.5	7.5		0
25.6	<4.2		−15

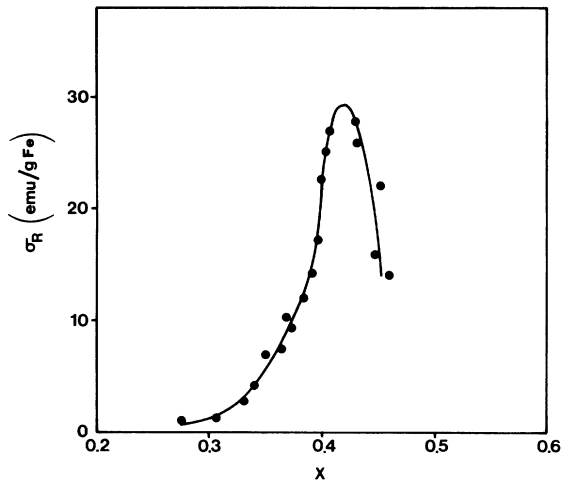

FIG. 5. Remanent magnetization measured at 4.2 K in Fe_xSn_{1-x} amorphous alloys.

$$\frac{1}{\chi}=\frac{1}{C}(T-\Theta)\,. \tag{7}$$

The paramagnetic Curie temperatures Θ are plotted versus alloy composition in Fig. 2 and happen to be zero near $x\simeq 0.27$. The C "constant" is not strongly composition dependent. For the sake of comparison the paramagnetic temperature Θ has always been obtained over the same temperature range, 100 to 300 K. When the isofield curves reach a well-defined maxima in their temperature-reversible part [see curve in Fig. 1(a)], it is also possible to determine a ferromagnetic temperature T_c as pictured in Fig. 1 corresponding to a classical ferro↔paramagnetic transition.

But the main feature worth reporting here is probably the evidence of an irreversibility behavior at low temperature for the less-iron-rich alloys. Looking, for instance, at Fig. 1(b), it is obvious that the susceptibility maximum does not correspond to a ferro↔paramagnetic transition: The high-temperature region is a temperature-reversible paramagnetic state indeed, but the low-temperature magnetization is strongly dependent on the sample's initial state. When cooled down to 4.2 K in a demagnetized state the magnetic moments are frozen in randomly distributed directions ($\sigma=0$). When progressively heated in an external field of 100 Oe, these magnetic moments have more and more tendency to align along the field (σ increases) until reaching a paramagnetic behavior (reversible Curie law for σ). If cooled back to 4.2 K, spins are refrozen but in a direction roughly corresponding to the maximum magnetization to be reached in the paramagnetic state. Then, the maximum of the magnetic susceptibility can be

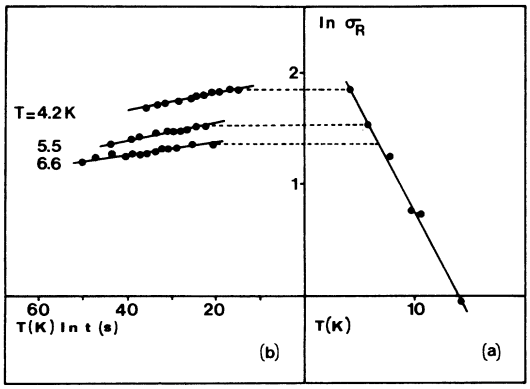

FIG. 6. (a) Temperature dependence of the remanent magnetization as measured in an $Fe_{0.35}Sn_{0.65}$ amorphous alloy after 60 sec. (b) Time-temperature correlation in remanent magnetization changes. It can be seen that $\ln\sigma_R$ extrapolates linearly to about 2.6 at $T=0$.

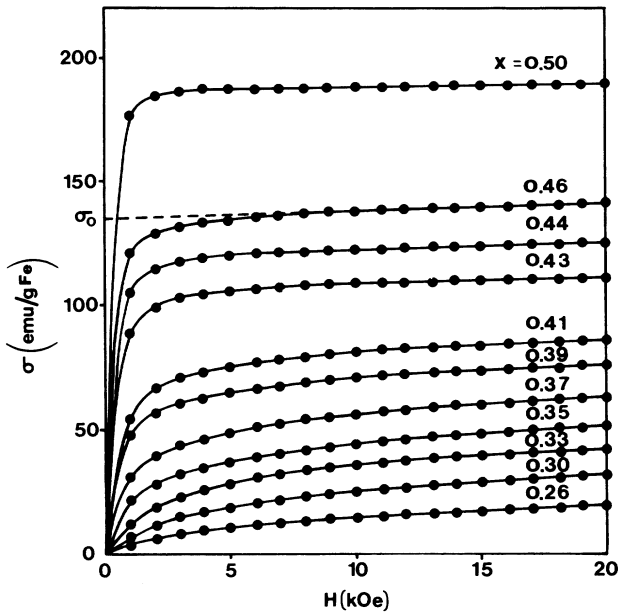

FIG. 7. Isothermal magnetization curves measured at 4.2 K in various Fe_xSn_{1-x} amorphous alloys using vibrating-sample magnetometer (within experimental accuracy error bars are smaller than thickness of drawing).

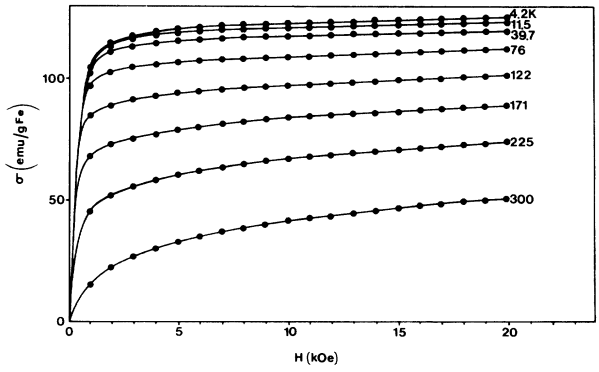

FIG. 8. Typical isothermal magnetization curves measured in $Fe_{0.45}Sn_{0.55}$ amorphous alloy at different temperatures (vibrating sample).

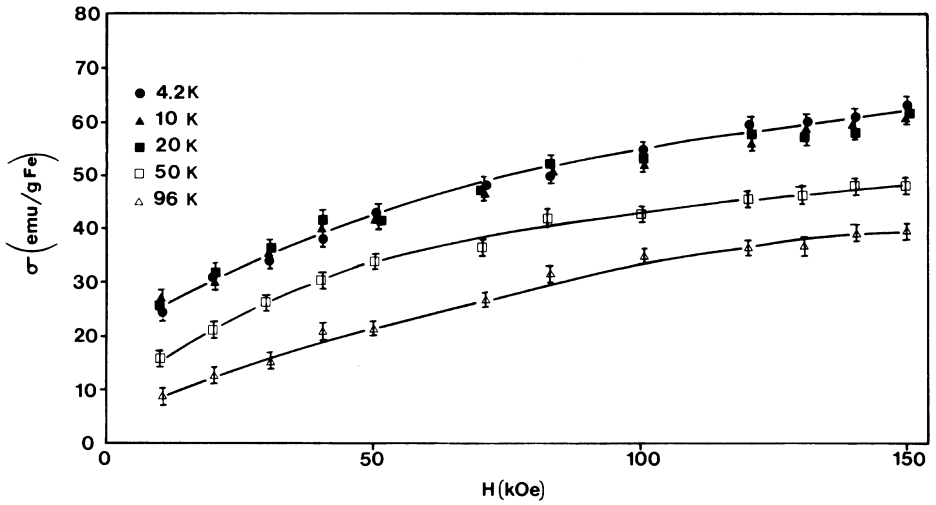

FIG. 9. Typical isothermal magnetization curves showing absence of saturation even in the high-field condition (here $x=0.30$). Data measured at $T=4.2$, 10, and 20 K are almost on the same curve within error bars (extraction method is less accurate by about a factor of 20 compared to vibrating-sample measurements).

assumed as corresponding to a blocking temperature T_G and in the following, T_G will be referred to as a temperature of "spin-glass ordering" even if the observed susceptibility maximum is not a true cusp. As expected from a spin-glass material, this susceptibility maximum in isofield curves progressively vanishes if stronger external fields are applied and does not exist any more if $H_{\text{ext}} \geq 3000$ Oe (see Fig. 3). Also the criticality predicted by Parisi *et al.*[23,24] is observed: In a fairly low-field condition a divergence occurs in the $\chi(H)$ behavior when measured near T_G. Proceeding further in analysis of the drawing data of the critical line $H(T)$, for instance, might be very tedious and is certainly beyond experimental accuracy.

Looking now at isofield magnetization curves typical of alloys containing slightly more iron [Fig. 1(a)] it can be seen that, as already stated, they exhibit a classical reversible transition between ferromagnetic and paramagnetic states. However, reminiscence of some kind of "spin-glass blocking" is also observed at a lower-temperature T_G. Such a reentrant spin-glass phase entered via a transition from a ferromagnetic state is still a question of active controversy. As far as the present paper is concerned, there is no point in discussing that since similar experimental behaviors are observed when the SG phase is entered via a transition from either a paramagnetic [Fig. 1(b)] or a ferromagnetic phase [Fig. 1(a)]. In both cases low-temperature irreversible behavior in $\sigma(T)$ curves is suppressed by increasing the applied field and the Parisi *et al.*[23,24] criticality is observed. Thus it is possible to present a multicritical phase diagram (Fig. 4) by plotting T_c and/or T_G as functions of iron concentration in the amorphous Fe_xSn_{1-x} alloys (see also Table I).

C. Hysteretic properties of the Fe_xSn_{1-x} alloys

High coercivity at low temperatures has been reported to be an identifying feature of a spin-glass-like state. The remanent magnetization σ_R measured in Fe_xSn_{1-x} amorphous alloys at $T=4.2$ K reaches a quite sharp maximum for a composition corresponding to $x \simeq 0.4$ (Fig. 5), which happens to be the triple point of the magnetic phase diagram (Fig. 4). The reported σ_R values have been obtained from samples previously magnetized under an applied field of 150 kOe, which unfortunately does not mean saturation in these materials. A second questionable point is how far the composition dependence of σ_R is not simply due to changes in T_G relative to 4.2 K; a proper answer to that question would be to determine $\sigma_R(0)$ by extrapolation of $\sigma_R(T)$ to $T=0$, which is not easily done with acceptable accuracy. However, that being the case, the observed maximum in the $\sigma_R(4.2\text{ K})$ curve (Fig. 5) is much sharper than the one in T_G (Fig. 4) and consequently must have some significance. In alloys corresponding to the lowest values of x ($x \simeq 0.30$), σ_R reaches a finite maximum at $T=0$ [Fig. 6(a)].

In fact, time and temperature dependences of the remanent magnetization are strongly correlated and must be described through a combined variable $T \ln t$ as shown by Prejean and Souletie,[18(a)] so that

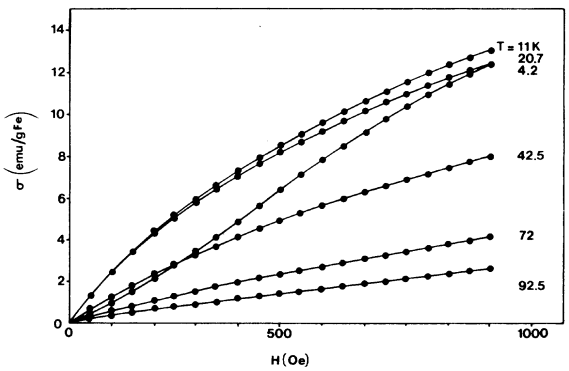

FIG. 10. In an $Fe_{0.33}Sn_{0.67}$ amorphous alloy the isothermal magnetization curves are not monotonous functions of T in their lowest-field part.

TABLE II. σ_0 and χ_0 values are given versus iron concentration.

x	σ_0 (emu/g Fe)	χ_0 (10^{-4} emu/cm^3)
0.50	185	1.09
0.46	136	3.02
0.45	122	3.8
0.43	108	4.4
0.41	79	7.0
0.40	80	7.05
0.39	69	6.5
0.37	52	9
0.35	40	8.2
0.33	30	8.5
0.30	20	
0.26	12	

$$\sigma_R(T,t)=\sigma_R^0\exp\left[-\frac{T}{T_0}\ln\left[\frac{t}{\tau_0}\right]\right]. \quad (8)$$

As shown in Fig. 6(b) the data fit the Prejean *et al.* time-temperature correlation in the low-temperature range reasonably well. The deduced relaxation time $\tau_0\simeq10^{-12}$ sec and $T_0\simeq150$ K are also comparable to the usual values observed in typical spin-glass material.[18(a),18(b)]

D. Magnetic isothermal curves

The field dependence of isothermal magnetization measured at 4.2 K in various Fe_xSn_{1-x} amorphous alloys up to $H=20$ kOe is shown in Fig. 7. For the highest values of iron concentration ($x\simeq0.45$–0.50 or more but not shown here) saturation of the magnetization σ_0 is easily reached. Then, σ_0 and the high-field susceptibility can be extracted from the linear parts of the magnetic isothermal curves. Changes in these isothermal curves upon temperature shifts are also monotonous as shown in Fig. 8.

When iron concentration is reduced, the following experimental features become less clear.

(i) Saturation of the magnetization cannot be achieved even with a magnetic field as large as 150 kOe (see curves in Fig. 9), and thus, determining σ_0 and χ_0 happens to be rather hazardous.

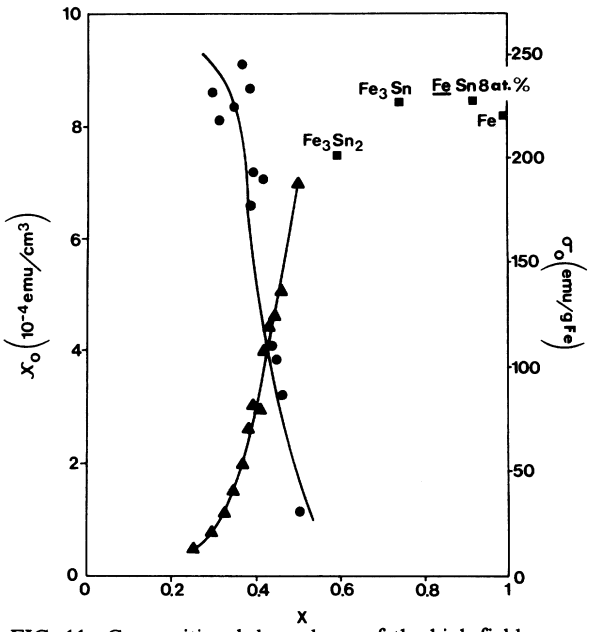

FIG. 11. Compositional dependence of the high-field susceptibility (●) and of the "saturation" magnetization as determined at 4.2 K in Fe_xSn_{1-x} amorphous alloys (▲). The σ_0 values for crystalline Fe-Sn compounds are also shown (■).

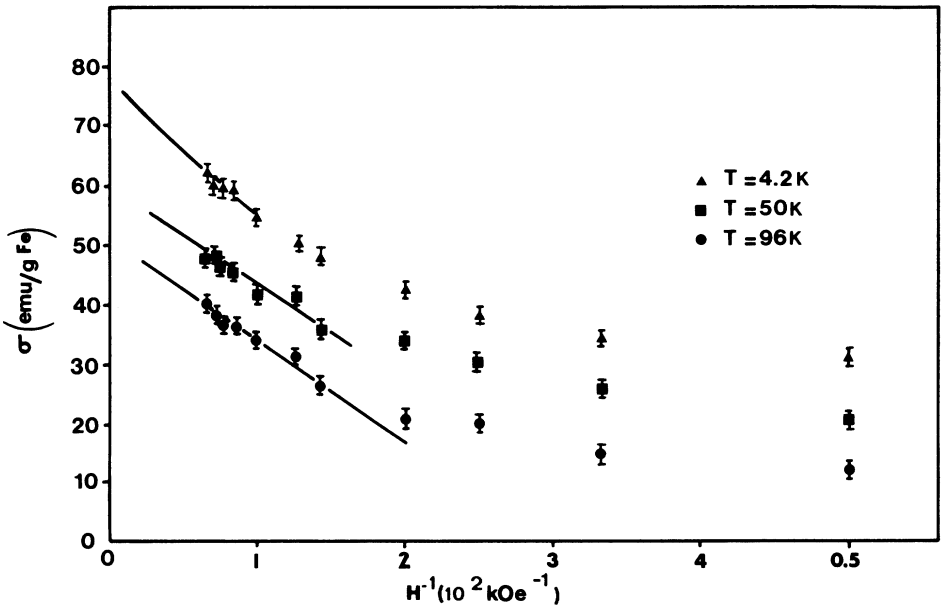

FIG. 12. Unsuccessfulness of a H^{-1} RKKY approach of the saturation in an $Fe_{0.30}Sn_{0.70}$ amorphous alloy. The σ data have been measured up to 150 kOe. Error bars are shown.

(ii) Isothermal magnetization is almost insensitive to temperature changes in the low-temperature range (up to about 20 K typically; see Fig. 9).

(iii) The magnetization is not a monotonous function of T in its low-field part (Fig. 10).

The σ_0 and χ_0 values are given in Table II and plotted versus iron concentration in Fig. 11. Because of difficulties in achieving saturation, the low-concentration part of these curves has to be considered very critically. The linear high-concentration part of $\sigma_0(x)$ when extrapolated to $\sigma_0=0$ gives a critical concentration $x_{cr}\simeq 0.35$ for the onset of long-range magnetic order in the Fe_xSn_{1-x} amorphous alloys.

III. DISCUSSION

It may be interesting to discuss the data reported in the preceding section by testing the various models of magnetic inhomogeneities summarized in the Introduction of this paper.

As developed in Sec. II B, the Fe_xSn_{1-x} amorphous alloys have a lot of common experimental features with spin-glass materials. However, mechanism involving long-range RKKY interaction between isolated magnetic atoms is not really expectable in such concentrated topologically disordered alloys. But similar interactions might be supposed to exist between distant clusters. In fact, this model is easily ruled out by plotting σ vs H^{-1}; according to expression (1), one should obtain straight lines with temperature-dependent slopes that converge to the same intersect with the ordinate axis. Obviously the $\sigma(H^{-1})$ curves as deduced from high-field data and shown in Fig. 12 do not fulfill the RKKY mechanism, even within the rather poor experimental accuracy.

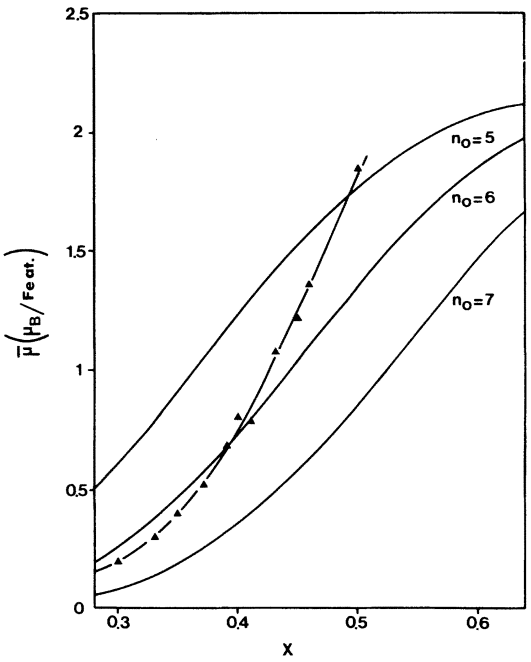

FIG. 13. Comparison of experimental data with magnetic moments values expected from a Jaccarino and Walker model.

A sensible approach would be to describe the onset of magnetism in these alloys through the appearance of giant moments due to the formation of "clusters" or favorable statistical arrangements of magnetic atoms. Intracluster interactions between iron atoms would be ferromagnetic while the intercluster interactions would be of the frustrat-

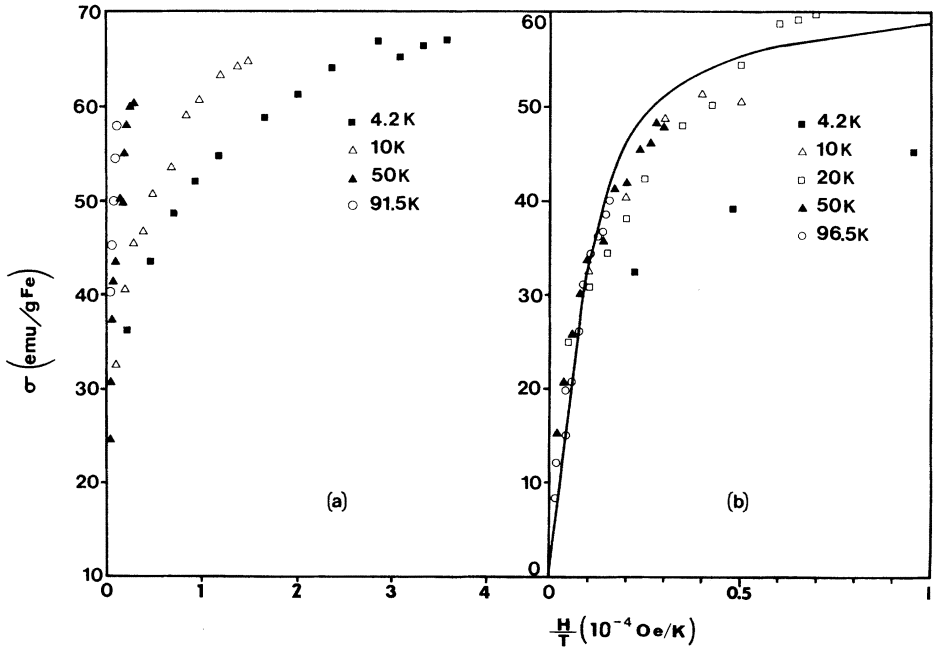

FIG. 14. (a) Unsuccessful and (b) partially successful fits of the experimental $\sigma(H/T)$ plots to the Langevin function for (a) $Fe_{0.33}Sn_{0.67}$ and (b) $Fe_{0.30}Sn_{0.70}$ amorphous alloys.

ed antiferromagnetic type through indirect Fe-Sn-Fe coupling[34] and would be responsible for the observed spin-glass behavior. Assuming that Sn and Fe atoms are randomly distributed in space and that a given iron atom has 12 nearest neighbors, it is possible to calculate an average magnetic moment $\bar{\mu}$ per iron atom using expression (2) in a Jaccarino-Walker model; $\mu(n)$ is given the value $2.2\mu_B$ if $n \geq n_0$ and 0 otherwise. Experimental $\bar{\mu}$ as deduced from $\sigma_0(x)$ data is compared to the calculated data in Fig. 13 for $n_0=5$–7. The total disagreement between experiments and theory strongly suggests that the structure of Fe_xSn_{1-x} amorphous alloys cannot be described in terms of dense random packing of hard spheres. However, if clusters of the Jaccarino-Walker type are then rejected, any other kind of possible clusters must be tested in attempted fits of σ vs H/T to the Langevin function [expression (3) in the Introduction]. In fact, fits of the $\sigma(H/T)$ high-field data to $\mathscr{L}$ functions are most generally impossible [see Fig. 14(a)] with only a very partial success in the case of low iron concentration ($x \simeq 0.30$) and data restricted to temperatures above 20 K [Fig. 14(b)]. Failure of the model is not really surprising since interactions between possible clusters make any attempt to describe the magnetization by a Langevin formalism very tedious. Therefore, clustering in the critical region cannot be definitively ruled out.

Assuming now that the observed spin-glass behavior might come from a fairly strong local anisotropy, randomly oriented through the material, and successfully competing with exchange interactions for some of the less-favored iron atoms, this should appear in a $(\sigma_0-\sigma)^{-1/2}$-vs-H plot of the high-field data.

As expected from Eq. (4) (see the Introduction), data happen to fit straight lines (see Fig. 15) within error bars. Deduced values of the apparent anisotropy field and of the constant A increase with temperature as shown in Table III.

In Eq. (4), H_0 and $\sqrt{A}$ can be written as

$$H_0(T)=\lambda\sigma_0(T)-\frac{2D}{\sigma_0(T)}\ ,$$
$$\sqrt{A}=\frac{|D|}{\sigma_0(T)}\ , \tag{9}$$

in which λ is the mean-field theory constant and D the anisotropy energy constant. Then

$$\frac{H_0}{\sqrt{A}}=\frac{\lambda\sigma_0^2(T)}{|D|}-2\frac{D}{|D|}\ .$$

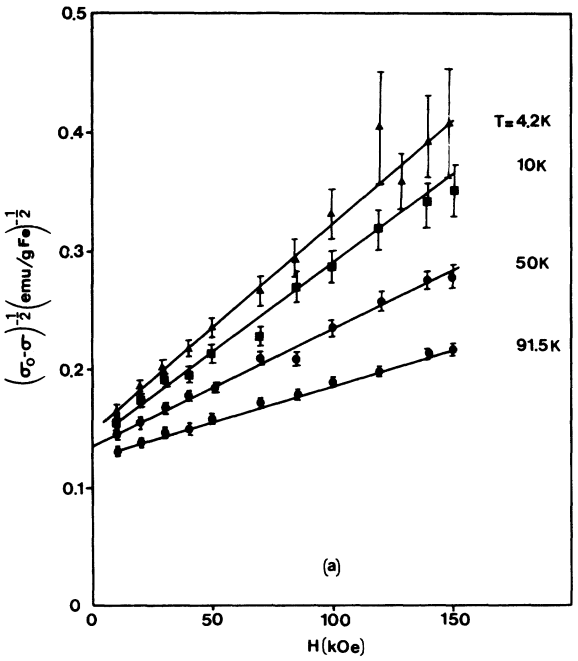

FIG. 15. Successful linear fits of the experimental $(\sigma_0-\sigma)^{-1/2}=f(H)$ plots for Fe_xSn_{1-x} alloys ($x=0.33$).

Data from Table III give $H_0/\sqrt{A} \simeq 0.15$ for alloy compositions within the critical region and up to $T \simeq 50$ K; at higher temperature $H_0/\sqrt{A}$ decreases slightly. These results are quite consistent with $\sigma_0(T)$ being always weak and a decreasing function of T. As H_0 increases with T (see Table III), Eq. (9) implies that D is negative. It is worth remembering that D is negative for easy plane of magnetization and positive for easy axis of magnetization, respectively.

Finally, models based on microscopic magnetic inhomogeneities or macroscopic disorder [Eqs. (5) and (6) in the Introduction] have been unsuccessfully tested through Arrots plots $\sigma^2=f(H/\sigma)$ (see Fig. 16) and $\sigma_0-\sigma$ vs $f(4\pi\sigma_0/H)$ (see Fig. 17), respectively. In particular, looking at the plot shown in Fig. 17, it can be clearly concluded that the studied alloys are quite well homogeneous at

TABLE III. Values of H_0 and $A^{1/2}$ for alloy compositions within the critical region.

T (K) \ x	0.33		0.37		0.40	
	$\sqrt{A}$ (kOe)	H_0 (kOe)	$\sqrt{A}$ (kOe)	H_0 (kOe)	$\sqrt{A}$ (kOe)	H_0 (kOe)
4.2	600	90	520	81	720	120
10	733	110				
50	1000	150	900	126	1170	190
100	1600	190	1860	230	3000	450
200					7500	975

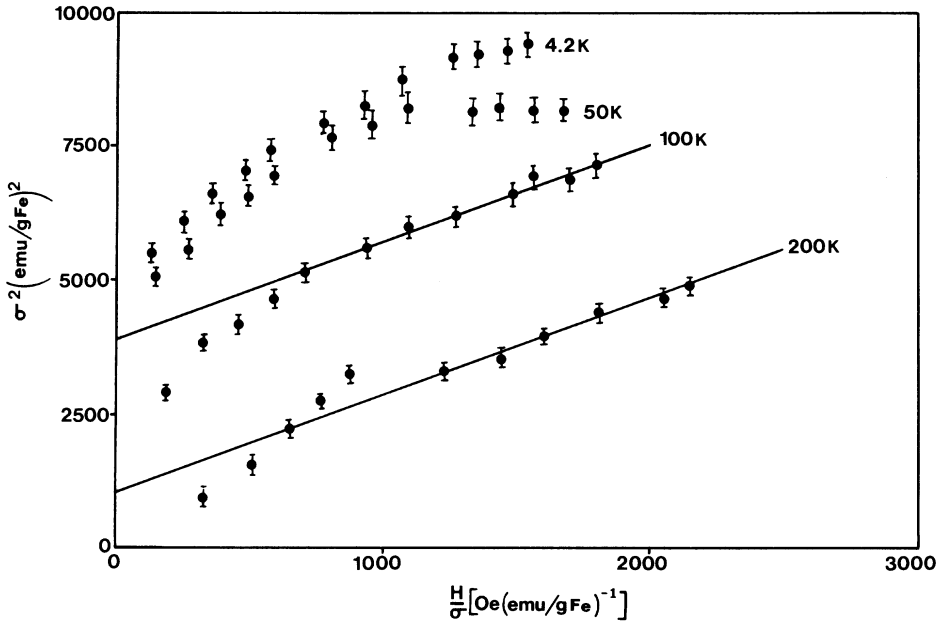

FIG. 16. Typical unsuccessful linear fits (even within error bars) of the experimental Arrots plots $\sigma^2(H/\sigma)$ for Fe_xSn_{1-x} amorphous alloys (here $x=0.40$).

macroscopic scale.

Therefore, the conclusion of this present section is that an explanation of the observed spin-glass-like behavior in an Fe_xSn_{1-x} amorphous alloys must be reasonably sought only in existence of local anisotropy effects and/or existence of magnetic clusters in the critical region. Obviously, this has to be understood in terms of the structural description of these alloys.

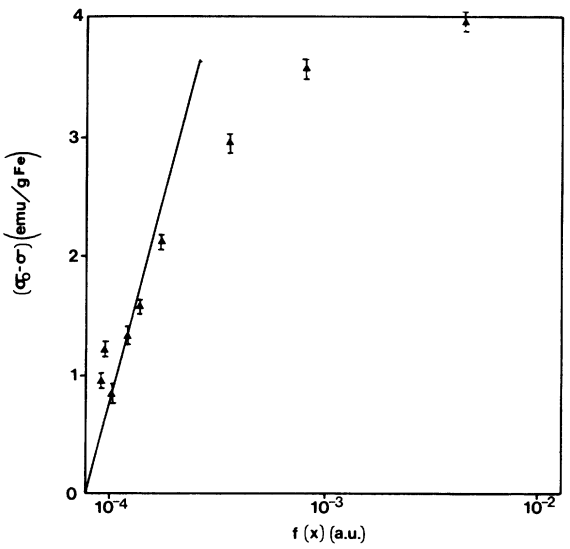

FIG. 17. Typical unsuccessful test (even within error bars) of a model of macroscopic magnetic inhomogeneity. Plot of $\sigma_0-\sigma$ vs $f(x)$ [$f(x)$ defined in text] for a $Fe_{0.37}Sn_{0.63}$ amorphous alloy.

IV. CONCLUSIONS

Bulk magnetic data as measured in Fe_xSn_{1-x} amorphous alloys, which have been obtained by the vapor-quenching method over quite a large compositional range, have resulted in the observation of a multicritical magnetic phase diagram. Spin-glass-like states, entered via a transition from either a paramagnetic or a ferromagnetic phase, have been suggested by irreversible behavior in the low-temperature part of the susceptibility measured under nearly-zero-field conditions and by the time-temperature dependence of the remanent magnetization.

High-magnetic-field data (up to 150 kOe) have shown that decreasing iron concentration around the critical composition in these iron-tin amorphous alloys results in making magnetic saturation impossible to achieve. Testing various descriptions of the influence of magnetic inhomogeneities suggests that the iron atoms which exhibit spin-glass-like behavior might be in magnetic clusters and experience a rather strong local anisotropy successfully competing with exchange interactions. Existence of such a strong local anisotropy had been previously suggested[35] by Mössbauer spectra recorded from a $Fe_{0.30}Sn_{0.70}$ amorphous alloy at 4.2 K with applied external magnetic field up to 60 kOe: Iron atoms experiencing a hyperfine field of about 130 kOe (then bearing magnetic moments of less than $1\mu_B$) do not modify the random orientation of their magnetic moments despite the strong applied external field.

More recently,[36] a detailed study of the same series of iron-tin amorphous alloys still using Mössbauer spectroscopy has been carried out: The relative concentrations of ferromagnetic and spin-glass iron atoms have been determined in function of the alloy composition. A structural model including description of short-range ordering and a phase-separation process is in progress.

[1]R. W. Cochrane, R. Harris, and M. J. Zuckermann, Phys. Rep. 48, 1 (1978).
[2]P. Monod and H. Bouchiat, J. Phys. (Paris) Lett. 43, L45 (1982).
[3]A. Berton, J. Chaussy, J. Odin, R. Rammal, and R. Tournier, J. Phys. (Paris) Lett. 43, L153 (1982).
[4]B. R. Coles, B. V. B. Sarkissian, and R. H. Taylor, Philos. Mag. 37, 489 (1978).
[5]J. Souletie and R. Tournier, J. Low Temp. Phys. 1, 95 (1969).
[6]R. Rammal and J. Souletie, *Les Houches Winter School on Magnetism,* edited by J. Alloul and M. Cyrot (North-Holland, New York, 1983).
[7]G. J. Nieuwenhuys, B. H. Verbeek, and J. A. Mydosh, J. Appl. Phys. 50, 1685 (1979).
[8]S. Kirkpatrick and D. Sherrington, Phys. Rev. B 17, 4384 (1978).
[9]E. P. Wolfarth, Physica 86B, 852 (1977).
[10]C. A. M. Mulder, A. J. Van Duyneveldt, and J. A. Mydosh, J. Magn. Magn. Mater. 15, 141 (1980).
[11]J. S. Schilling, P. J. Ford, U. Larsen, and J. A. Mydosh, Phys. Rev. B 14, 4368 (1976).
[12]G. Dublon, Phys. Status Solidi A 60, 287 (1980).
[13]J. Durand, Rev. Phys. Appl. 15, 1036 (1980).
[14]Y. Yeshurun, M. B. Salamon, K. V. Rao, and H. S. Chen, Phys. Rev. Lett. 45, 1366 (1980).
[15]G. Dublon and Y. Yeshurun, Phys. Rev. B 25, 4899 (1982).
[16]G. Aeppli, S. M. Shapiro, R. J. Birgeneau, and H. S. Chen, Phys. Rev. B 25, 4882 (1982).
[17]J. L. Tholence and R. Tournier, J. Phys. (Paris), Colloq. 35, C4-229 (1974).
[18](a) J. L. Prejean and J. Souletie, J. Phys. (Paris) 41, 1335 (1980); (b) H. Bouchiat and P. Monod, J. Magn. Magn. Mater. 30, 175 (1982).
[19]C. N. Guy, J. Phys. F 7, 1505 (1977).
[20]F. W. Smith, Phys. Rev. B 10, 2980 (1974).
[21]A. Larkin and D. E. Khmel'Nitskii, Zh. Eksp. Teor. Fiz. 58, 1789 (1970) [Sov. Phys.—JETP 31, 958 (1970)].
[22]M. D. Nunez-Regueiro and K. Matho, J. Phys. F 12, 1013 (1980).
[23]G. Parisi and G. Toulouse, J. Phys. (Paris) Lett. 41, L361 (1980).
[24]J. Vannimenus, G. Toulouse, and G. Parisi, J. Phys. 42, 565 (1981).
[25]V. Jaccarino and L. R. Walker, Phys. Rev. Lett. 15, 258 (1965).
[26]T. Kaneyoshi, Internal Report No. 13-79, Department of Physics, Nagoya University, Japan (unpublished).
[27]E. Callen, Y. J. Liu, and J. R. Cullen, Phys. Rev. B 16, 263 (1977).
[28]H. Kronmuller, J. Phys. (Paris), Colloq. 41, C8-618 (1980).
[29]D. M. Edwards, in *Electrons in Disordered Metals and at Metallic Surfaces,* edited by D. L. Gyorffy and L. Sheire (Plenum, New York, 1979), p. 76.
[30]A. Aharony and E. Pytte, Phys. Rev. Lett. 45, 1583 (1980).
[31]L. Neel, J. Phys. Radium 9, 184 (1948).
[32]B. Rodmacq, M. Piecuch, Chr. Janot, G. Marchal, and Ph. Mangin, Phys. Rev. B 21, 1911 (1980).
[33]J.-F. Geny, G. Marchal, Ph. Mangin, Chr. Janot, and M. Piecuch, Phys. Rev. B 25, 7449 (1982).
[34]D. Teirlinck, M. Piecuch, J.-F. Geny, G. Marchal, Ph. Mangin, and Chr. Janot, IEEE Trans. Magn. 17, 3079 (1981).
[35]S. Nikolov, M. Piecuch, G. Marchal, and Chr. Janot, J. Phys. (Paris), Colloq. 41, C8-666 (1980).
[36]Chr. Janot, M. Piecuch, G. Marchal, D. Teirlinck, and M. Vergnat, in *Proceedings of the Second International Conference on the Structure of Non-Crystalline Materials, Cambridge, 1982,* edited by P. H. Gaskell, J. M. Parker, and E. A. Davis (Taylor and Francis, London, 1983), p. 234.